JOURNAL OF APPLIED ELECTROCHEMISTRY **27** (1997) 235–239

Synthesis and electrochemical properties of new viologen polymers

M. LIEDER*, C. W. SCHLÄPFER

Institute of Inorganic Chemistry, University of Fribourg, CH-1700 Fribourg, Switzerland

Received 4 April 1996; revised 27 June 1996

New polymeric viologens containing tetra-, tri-, or diethylglycol links as 1,1′-substituents has been synthesized by the reaction of tosylated ethylglycols with dipyridine in *N, N*-dimethylformamide (DMF). Thin films of insoluble hexafluorophosphate salts of these polyviologens were examined using electrochemical technique, electrochemical quartz crystal microbalance (EQMB), and atomic force microscopy (AFM). The cyclovoltammetric results show that the composition of the polyviologen determines the kinetics of the redox reactions and the mode of the charge transport through the film. The charge compensation during the reduction process is accomplished by cation insertion, and vice versa during oxidation. However, the EQMB data indicate that some anion insertion during oxidation also takes place. Water movement during the redox processes was observed.

1. Introduction

Viologens, 1,1′-disubstituted-4,4′-dipyridinium ions and their polymeric analogues have been studied intensively since their discovery in 1993 [1] mainly due to emergence of new applications. Viologens were originally investigated as redox indicators in biological studies [1] in view of their low redox potentials and good reversibility. Subsequently, some of their derivatives, known as paraquats were found to have herbicidal activity [2]. Later there were many fundamental and applied studies on their electrochromic properties [3]. More recently they have been used as electroactive layers to modify electrode surfaces [4, 5] and as electrode materials for batteries [6].

The electrochemical properties of viologens are strongly influenced by 1,1′-substituents which affect the solubility of the cation radical and the reversible potential of both reduction steps. Variants of these substituents have been thoroughly studied in relation to the electrochromic behaviour of viologen [7].

In this paper we report on synthesis and some electrochemical properties of new polymeric viologens containing ethylglycol links as 1,1′-substituents which should render the polyviologen chains more hydrophilic and flexible than their analogues containing alkyl substituents. As the separation distance between the redox centres on the viologen units may lead to their interactions [8] we used three different substituents containing two, three and four ethylglycol segments. The synthesized polyviologens were converted into insoluble salts and then deposited as thin film on a glassy carbon support.

Cyclic voltammetry was used to examine the reversibility of the redox reactions in the films. Charge and solvent transport across the film/solution interface was studied by the electrochemical quartz microbalance (EQCM) technique. Changes in the film volume were studied by the atomic force microscopy (AFM).

2. Experimental details

2.1. *Materials and synthesis*

All solutions were made from deionized water which had been further purified by distillation. The following chemicals obtained from Aldrich and Fluka were used without further purification: $LiClO_4$, *N,N*-dimethylformamide (DMF), diethylene glycol di-*p*-tosylate, 98% (dg), triethylene glycol di-*p*-tosylate, 98% (trg), tetraethylene glycol di-*p*-tosylate, 97% (tg), and 4,4′-dipyridyl (dipy). A variety of polyviologen polymers were conventionally obtained by the reaction of tosylated ethylglycols with dipyridine at room temperature in DMF [9]. These polymers contained tosylate anion and were soluble in water. They were converted into insoluble hexafluorophosphate salts by precipitation from aqueous solution with an excess of $NaPF_6$. The high resolution ^{1}H-NMR spectrum of the polyviologens allowed two doublets at 9.05 and 8.52 ppm to be distinguish which were assigned to the symmetrically disubstituted dipyridyl unit and four doublets at 8.91, 8.40, 8.05 and 7.65 ppm which were assigned to the terminal, monosubstituted dipyridyl. There are also four doublets at 4.85, 4.05, 3.7 and 3.6 ppm for tetraethylglycol viologen (TEGV), three doublets at 4.88, 4.05 and 3.65 ppm for triethylglycol viologen (TRIEGV) and two doublets at 4.89 and 4.05 ppm for diethylglycol viologen (DEGV) which

---

[*] On leave from The Technical University of Gdansk, Department of Chemistry, Narutowicza 11/12, 80-952 Gdansk, Poland

0021-891X

Table 1. Composition of the condensation products between tosylated ethylglycols and 4,4′-dipyridine

Polymer	*sym : asym*	*N : F*	*sym : tos*	*Number of units*
TEGV	2.8 : 1	1 : 5	13 : 1	5 dipy 4tg
TREGV	9.4 : 1	1 : 6	12.8 : 1	11 dipy 10 trg
DEGV	0.6 : 1	1 : 3	4.4 : 1	3 dipy 2 dg

sym = symmetrically disubstituted dipyridyl
asym = monosubstituted dipyridyl
N : F = molar ratio of nitrogen to fluorine atoms in the polymer.
sym : tos = molar ratio of symmetrical dipyridyl to tosylate end groups.

were assigned to the –CH_2O– group. In addition two weak doublets at 7.5 and 7.8 ppm were observed and assigned to tosylate end groups.

Based on elemental analysis and ^{1}H-NMR we determined the composition of the studied polyviologens. The results are shown in Table 1. Molar ratios of charged nitrogen sites on each polymer to hexafluorophosphate anions were close to 1:1.

2.2. *Electrode coating procedure*

A vitreous carbon disc (0.08 cm^2), set in a Teflon tube was used as working electrode. Fresh electrode surfaces were produced by polishing with diamond paste. In order to improve adhesion the carbon electrode was immersed in a solution of chlorosulfonic acid in dichloromethane for a few minutes, then rinsed with distilled water. This treatment is believed to create polar functional groups on the carbon surface [10].

A 1% (w/v) polymer spincoating solution was prepared in 45 : 5 : 50 vol % HCl + H_2O + dioxan [11]. A few drops (1.5–10 μl) of the stock solution were spread by a micropipette on the electrode surface and the solvents were allowed to evaporate under continuous rotation at 500 rpm. The thickness of the coating films was estimated from the amount of polymer applied, assuming that its swollen density was 1 g cm^{-3}.

2.3. *Apparatus and procedures*

The EQCM setup consisted of a quartz crystal 5 MHz ‘AT-cut’ (13 mm dia.) covered with a gold film (100 nm thick) with an area of 0.36 cm^2, the PAR 273 potentiostat and a universal counter (Tabor Electronics 6030) for measuring the resonance frequency. The working electrode was isolated from ground by two inductively coupled coils. Current, mass and frequency change signals, *f*, were recorded on an X–Y recorder (BBC SE780). An Hg_2SO_4/K_2SO_4 electrode was used as reference and a Pt wire as auxiliary electrode. Rigid layer behaviour of the film was confirmed by linearity of the global mass change with the charge stored in the film for different thickness [12]. The proportionality constant relating the calculated mass changes to the experimentally observed frequency changes is 47.6 Hz cm^2 μg^{-1} for our instrument. For quantitative evaluation of the mass change from the EQCM data, two approaches are recommended [12]: (i) using the extreme points in charge and frequency for each redox step or (ii) using the slopes of the charge–frequency plot. Although, the latter approach is more precise [12] it could not be applied due to directional hysteresis and non-linearity of the plots caused by the nonequilibrium state of the mobile species during the redox reaction.

In situ AFM images of the polymer film / electrolyte interface during electrochemical polarization were taken using a Nanoscope III (Digital Instruments Inc., Santa Barbara CA). The electrochemical cell consisted of a commercial cuvette equipped with the SCE reference electrode and a Pt counter-electrode. The potentials were controlled by a PAR 173 potentiostat with a PAR 175 waveform generator.

Cyclic voltammograms (CV) were obtained with a PAR 170/270 system. A one compartment electrochemical cell containing the working electrode, a Pt mesh, and the SCE reference electrode was used. The electrochemical characterization of the films was carried out in contact with $LiClO_4$ solutions. Argon was bubbled through the solution before the measurements. All potentials in the paper are reported relative to the saturated calomel electrode (SCE). Experiments were conducted at ambient laboratory temperature.

3. Results and discussion

3.1. *Cyclic voltammetry*

Typical cyclic voltammograms for three studied polymers are shown in Fig. 1. The CV for the TEGV polymer (curve 1) resembles an immobilized redox layer response with the following parameters: $\delta \log j_{pc} / \delta \log v = 0.88$, $\delta \log j_{pa} / \delta \log v = 0.90$, $j_{pc}/j_{pa} = 1$, and

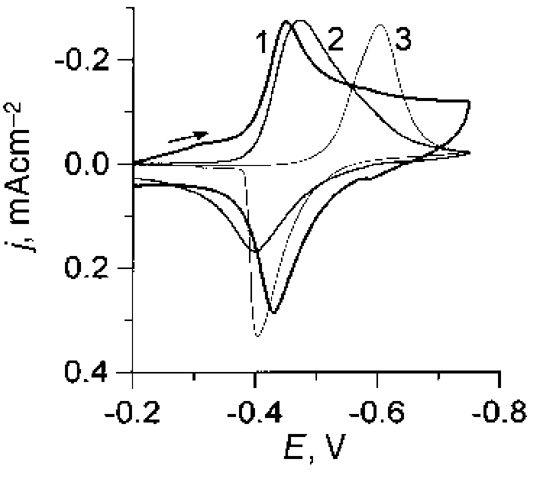

Fig. 1. Cyclic voltammetry of the electrode modified with a 1 μm film of (1) TEGV; (2) TRIEGV; (3) DEGV in 0.1 M $LiClO_4$; $v = 0.01$ V s^{-1}.

full width at half-maximum, FWHM = 0.090V, which indicates that all the redox sites have the same effective E^0_{surf} and their activities can be approximated with the surface quantities Γ_{ox} and Γ_{red} [13]. The cathodic and anodic peak separation does not exceed 0.02 V and the curve preserves its symmetry even at a sweep rate as high as 1 V s^{-1}.

A diffusion-like response for TRIEGV film (curve 2) is semi-reversible at low sweep rates ($\delta \log j_{pc,a}$ / $\delta \log v = 0.53$, $\delta \log j_{pa} / \delta \log v = 0.48$, $j_{pc}/j_{pa} = 0.62$). At higher sweep rates, however, the mass change becomes irreversible and the peak separation increases due to the influence of the film resistance on the charge carrier and/or counter ion movement. The slow diffusion of this polymer is caused by its relatively large molecular weight (Table 1).

Both peaks for DEGV polymer are non-symmetrical (curve 3), with the reduction peak shifted negatively and currents for the oxidation resembling phaselike behaviour (sharp peak falling). This may imply precipitation or adsorption of the reduced compound. On scan reversal, however, we did not observe accumulation of the reduced product. The peak potential and peak width of the oxidation and reduction waves are very sensitive to potential scan rate. A log–log plot of peak current against scan rate for the oxidation had a slope of 0.42. ($\delta \log j_{pc} / \delta \log v = 0.42$, $\delta \log j_{pa} / \delta \log v = 0.37$). It is worth noting that, according to Table 1, DEGV, which is composed of three dipyridyl and two diethylglycol units, was the smallest molecule studied.

Figure 2 shows the CV response for TEGV polymer to a scan over both redox processes. The cathodic peak for the second step indicate diffusion-like characteristics and the lower currents which indicate a decrease in the charge transfer kinetics. This may be an outcome of the dilution of the redox centres in the film due to solvent intake during polarization. In order to confirm this assumption quartz microbalance experiments were carried out.

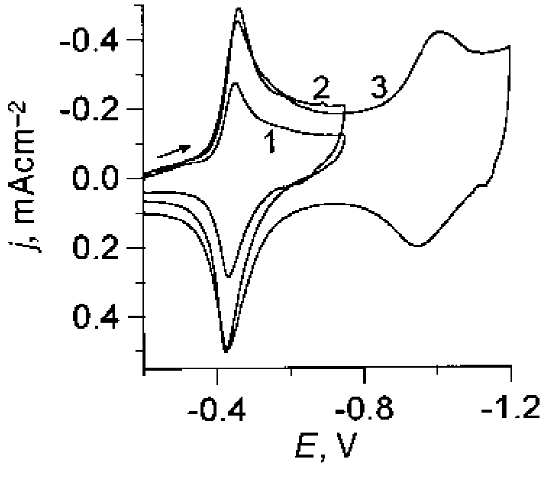

Fig. 2. Cyclic voltammetry of the electrode modified with a 1 μm film of TEGV in 0.1 M $LiClO_4$. Sweep rate: (1) 0.01, (2) and (3) 0.05 V s^{-1}.

3.2. *Quartz microbalance*

Interphase motion involving ions and solvent crossing the boundary film/external solution during a potential cycle was observed by the EQMB technique. The EQMB frequency data and a simultaneously recorded CV for the TEGV film are shown in Fig. 3. The beginning of the electrochemical reaction indicated by an increase in the current (upper curve) is followed, with negligible delay, by a strong frequency decrease (lower curve) interpreted as mass increase [12]. The electrode becomes heavier because it incorporates ions and solvent molecules from the surrounding solution due to redox processes in the film. On backward polarization (oxidation processes) these 'guest' molecules leave the polymer what results in the frequency increase until the initial level is reached. The mass changes that occur during oxidation or reduction of the film may be caused by the transport of anions, cations and solvent [12]. The contribution of the particular species may vary during polarization due to changes in the oxidation state of the polymer [14, 15] and the transition of the affinity of the polymer to solvent molecules. The observed frequency decrease during the reduction process indicates that the inflow of cations from the supporting electrolyte, compensating the decreasing charge of the dipyridyl cations takes place. During the backward sweep an interesting local minimum at −0.45 V in the frequency curve, corresponding with the anodic CV peak (upper curve) can be seen. This minimum can not be explained by the cations movement. It seems that at this point of the oxidation process the

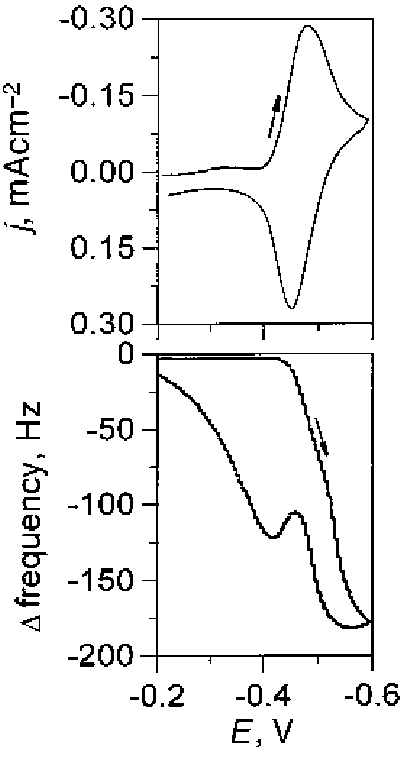

Fig. 3. Cyclic voltammogram (top), and EQCM frequency response (bottom) of the electrode modified with the 1 μm TEGV film in 0.1 M $LiClO_4$; $v = 0.01$ V s^{-1}.

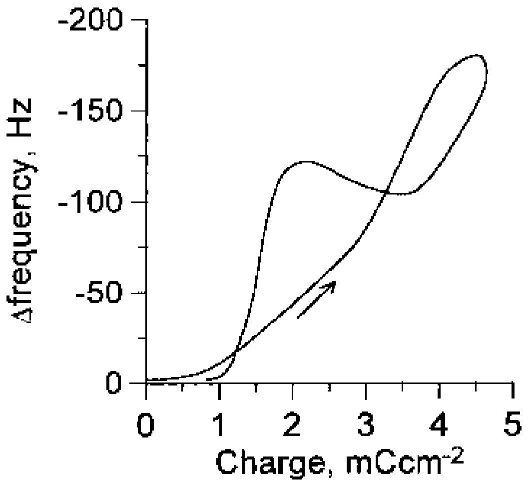

Fig. 4. EQCM frequency plot collected simultaneously with voltammogram in Fig. 3.

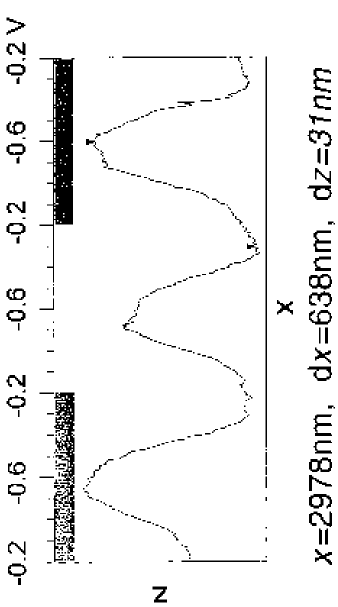

Fig. 5. Thickness profile of the 1 μm TEGV film in 0.1 M $LiClO_4$ measured during simultaneous electrochemical-AFM experiment. The potentials in the upper side of the graph show one and a half potential cycle; $v = 0.01$ V s^{-1}. The dx and dz denote the horizontal and vertical distances between marked points, respectively.

cation egress is too slow to follow the polymer charge changes. Therefore, some additional ingress of anions takes place which allows to preserve the charge balance in the film. These anions cause the temporarily frequency decrease.

Cations and anions are driven across the film/solution interface by the charge compensation necessity, whereas postulated earlier solvent transport is a consequence of the difference in the thermodynamic activity of the solvent inside and outside of the film [16]. The question of the water movement can be resolved by calculating the apparent molar mass MW from a plot of frequency changes vs. the total charge passed during polarization. The plot for the first reduction step of the TEGV film (Fig. 4) yields $MW = 79$ g mol^{-1} which is larger than the molar mass of Li (7 g mol^{-1}). It indicates that solvent, approximately 4 H_2O per 1 Li^+, is transported into the film during the intake of the cations. This finding is consistent with the *in situ* AFM results, Fig. 5, showing that the film expands reversibly on reduction and then shrinks to its initial volume on oxidation. The maximum increase in the film height was observed at a potential of −0.6 V. Unfortunately, it is impossible to estimate the extent of swelling caused by the redox reactions because the film incorporates solvent prior to polarization and its dry thickness (1 μm) is no longer valid.

Two remaining polymers TRIEGV and DEGV also undergo volume change during electrochemical polarization and their EQMB characteristics resemble that for the TEGV polymer. However, the quantitative comparison of the amount of water entering each polymer during polarization turned out to be impossible due to the nonrigid layer behaviour of the TRIEGV and DEGV films.

4. Conclusions

It was found that the redox processes in the polyviologen films, as well as the mode of the charge transport through these films, are determined by their composition, in particular, by the degree of polymerization of the polyviologen matrix, and the number of ethylglycol units in the substituent. It was also found that the redox processes in the polyviologen films are accompanied by the interface ion and solvent movement. The latter movement leads to the dilution of the redox centres resulting in a decrease in the reaction kinetics. Finally, a mixed ion transport (simultaneous cation expulsion and anion insertion) for the oxidation reaction was observed.

Acknowledgement

We wish to thank Drs O. Haas and R. Kötz (Paul Scherrer Institute, Switzerland) for the Quartz Microbalance, and Prof. H. Siegenthaler, University of Bern for AFM measurements. This work was supported by Bundesamt für Energiewirtschaft EF-Proc (89) 023.

References

[1] L. Michaelis and E. S. Hill, *J. Gen. Physiol.* **16** (1933) 859.
[2] L. A. Summers, 'The Bipyridinium Herbicides', Academic Press, New York (1980).
[3] P. M. S. Monk, R. J. Mortimer and D. R. Rosseinsky, 'Electrochromism: Fundamentals and Applications', VCH, Weinheim, (1995), p. 124.
[4] G. Inzelt, *in* 'Electroanalytical Chemistry', vol. 18 (edited by A. J. Bard), Marcel Dekker, New York (1994).
[5] G. S. Ostrom and D. A. Buttry, *J. Phys. Chem.* **99** (1995) 15 236.
[6] A. Bouridah, F. Dalard and M. Armand, *Solid State Ionics* **28–30** (1988) 950.
[7] C. L. Bird and A. T. Kuhn, *Chem. Soc. Rev.* **10** (1981) 49.
[8] A. Deronzier, B. Galland and M. Vieira, *Nouveau J. Chim.* **6** (1982) 97.

[9] T. Endo, A. Kameyama, Y. Mambu, Y. Kashi and M. Okawara, *J. Polym. Sci. Polym. Chem. Ed.* **28** (1990) 2509.

[10] E. T. T. Jones and L. R. Faulkner, *J. Electroanal. Chem.* **222** (1987) 201.

[11] H. Akahoshi, S. Toshima and K. Itaya, *J. Phys. Chem.* **85** (1981) 818.

[12] D. A. Buttry in H. D. Abruña (Ed.), 'Electrochemical Interfaces. Modern Techniques for In Situ Interface Characterization', VCH, New York (1991).

[13] R. W. Murray, *in* R. W. Murray (Ed.), 'Techniques of Electrochemistry. Molecular Design of Electrode Surfaces', vol. 22, Wiley & Sons New York (1992).

[14] M. Lieder and C. W. Schläpfer, *J. Electroanal. Chem.*, **411** (1996) 87.

[15] J. H. Kaufman, K. K. Kanazawa and G. B. Street, *Phys. Rev. Lett.*, **53** (1984) 2461.

[16] F. Helfferich, 'Ion Exchange', McGraw-Hill, New York (1962).